

Wave front engineering from an array of thin aperture antennas

Ming Kang,^{1,2} Tianhua Feng,^{1,3} Hui-Tian Wang,^{2,4} and Jensen Li^{1,3,*}

¹ Department of Physics and Materials Science, City University of Hong Kong, Tat Chee Avenue, Kowloon Tong, Hong Kong, China

² School of Physics and Key Laboratory of Weak Light Nonlinear Photonics, Nankai University, Tianjin 300071, China

³ State Key Laboratory of Millimeter Waves, City University of Hong Kong, Tat Chee Avenue, Kowloon, Hong Kong, China

⁴National Laboratory of Solid State Microstructures, Nanjing University, Nanjing 210093, China
[*jensen.li@cityu.edu.hk](mailto:jensen.li@cityu.edu.hk)

Abstract: We propose an ultra-thin metamaterial constructed by an ensemble of the same type of anisotropic aperture antennas with phase discontinuity for wave front manipulation across the metamaterial. A circularly polarized light is completely converted to the cross-polarized light which can either be bent or focused tightly near the diffraction limit. It depends on a precise control of the optical-axis profile of the antennas on a subwavelength scale, in which the rotation angle of the optical axis has a simple linear relationship to the phase discontinuity. Such an approach enables effective wave front engineering within a subwavelength scale.

©2012 Optical Society of America

OCIS codes: (160.3918) Metamaterials; (260.2110) Electromagnetic optics; (310.6860) Optical properties.

References and links

1. R. A. Shelby, D. R. Smith, and S. Schultz, "Experimental verification of a negative index of refraction," *Science* **292**(5514), 77–79 (2001).
2. S. Zhang, Y. S. Park, J. Li, X. Lu, W. Zhang, and X. Zhang, "Negative refractive index in chiral metamaterials," *Phys. Rev. Lett.* **102**(2), 023901 (2009).
3. J. B. Pendry, D. Schurig, and D. R. Smith, "Controlling electromagnetic fields," *Science* **312**(5781), 1780–1782 (2006).
4. J. Li and J. B. Pendry, "Hiding under the carpet: a new strategy for cloaking," *Phys. Rev. Lett.* **101**(20), 203901 (2008).
5. N. I. Landy, S. Sajuyigbe, J. J. Mock, D. R. Smith, and W. J. Padilla, "Perfect metamaterial absorber," *Phys. Rev. Lett.* **100**(20), 207402 (2008).
6. H. T. Chen, J. Zhou, J. F. O'Hara, F. Chen, A. K. Azad, and A. J. Taylor, "Antireflection coating using metamaterials and identification of its mechanism," *Phys. Rev. Lett.* **105**(7), 073901 (2010).
7. V. A. Fedotov, P. L. Mladyonov, S. L. Prosvirnin, A. V. Rogacheva, Y. Chen, and N. I. Zheludev, "Asymmetric propagation of electromagnetic waves through a planar chiral structure," *Phys. Rev. Lett.* **97**(16), 167401 (2006).
8. D. H. Kwon, P. L. Werner, and D. H. Werner, "Optical planar chiral metamaterial designs for strong circular dichroism and polarization rotation," *Opt. Express* **16**(16), 11802–11807 (2008).
9. N. Yu, P. Genevet, M. A. Kats, F. Aieta, J. P. Tetienne, F. Capasso, and Z. Gaburro, "Light propagation with phase discontinuities: generalized laws of reflection and refraction," *Science* **334**(6054), 333–337 (2011).
10. N. Engheta, "Antenna-Guided Light," *Science* **334**(6054), 317–318 (2011).
11. X. Ni, N. K. Emani, A. V. Kildishev, A. Boltasseva, and V. M. Shalaev, "Broadband light bending with plasmonic nanoantennas," *Science* **335**(6067), 427 (2012).
12. F. Aieta, P. Genevet, N. Yu, M. A. Kats, Z. Gaburro, and F. Capasso, "Out-of-plane reflection and refraction of light by anisotropic optical antenna metasurfaces with phase discontinuities," *Nano Lett.* **12**(3), 1702–1706 (2012).
13. P. Genevet, N. Yu, F. Aieta, J. Lin, M. A. Kats, R. Blanchard, M. O. Scully, Z. Gaburro, and F. Capasso, "Ultra-thin plasmonic optical vortex plate based on phase discontinuities," *Appl. Phys. Lett.* **100**(1), 013101 (2012).
14. F. Gori, "Measuring Stokes parameters by means of a polarization grating," *Opt. Lett.* **24**(9), 584–586 (1999).
15. L. Marrucci, C. Manzo, and D. Paparo, "Optical spin-to-orbital angular momentum conversion in inhomogeneous anisotropic media," *Phys. Rev. Lett.* **96**(16), 163905 (2006).
16. R. Blanchard, G. Aoust, P. Genevet, N. Yu, M. A. Kats, Z. Gaburro, and F. Capasso, "Modeling nanoscale V-shaped antennas for the design of optical phased arrays," *Phys. Rev. B* **85**(15), 155457 (2012).
17. T. W. Ebbesen, H. J. Lezec, H. F. Ghaemi, T. Thio, and P. A. Wolff, "Extraordinary optical transmission through sub-wavelength hole arrays," *Nature* **391**(6668), 667–669 (1998).

18. F. J. Garcia-Vidal, L. Martin-Moreno, T. W. Ebbesen, and L. Kuipers, "Light passing through subwavelength apertures," *Rev. Mod. Phys.* **82**(1), 729–787 (2010).
19. F. J. García-Vidal, E. Moreno, J. A. Porto, and L. Martín-Moreno, "Transmission of light through a single rectangular hole," *Phys. Rev. Lett.* **95**(10), 103901 (2005).
20. R. Gordon, A. G. Brolo, A. McKinnon, A. Rajora, B. Leathem, and K. L. Kavanagh, "Strong polarization in the optical transmission through elliptical nanohole arrays," *Phys. Rev. Lett.* **92**(3), 037401 (2004).
21. Z. Ruan and M. Qiu, "Enhanced transmission through periodic arrays of subwavelength holes: the role of localized waveguide resonances," *Phys. Rev. Lett.* **96**(23), 233901 (2006).
22. N. Dahan, Y. Gorodetski, K. Frischwasser, V. Kleiner, and E. Hasman, "Geometric Doppler effect: spin-split dispersion of thermal radiation," *Phys. Rev. Lett.* **105**(13), 136402 (2010).
23. J. Pendry, A. Holden, D. Robbins, and W. Stewart, "Magnetism from conductors and enhanced nonlinear phenomena," *IEEE Trans. Microw. Theory Tech.* **47**(11), 2075–2084 (1999).
24. C. Enkrich, M. Wegener, S. Linden, S. Burger, L. Zschiedrich, F. Schmidt, J. F. Zhou, T. Koschny, and C. M. Soukoulis, "Magnetic metamaterials at telecommunication and visible frequencies," *Phys. Rev. Lett.* **95**(20), 203901 (2005).
25. N. Liu, H. Liu, S. N. Zhu, and H. Giessen, "Stereometamaterials," *Nat. Photonics* **3**(3), 157–162 (2009).
26. I. Sersic, M. Frimmer, E. Verhagen, and A. F. Koenderink, "Electric and magnetic dipole coupling in near-infrared split-ring metamaterial arrays," *Phys. Rev. Lett.* **103**(21), 213902 (2009).
27. L. T. Vuong, A. J. L. Adam, J. M. Brok, P. C. M. Planken, and H. P. Urbach, "Electromagnetic spin-orbit interactions via scattering of subwavelength apertures," *Phys. Rev. Lett.* **104**(8), 083903 (2010).
28. S. Zhang, D. A. Genov, Y. Wang, M. Liu, and X. Zhang, "Plasmon-induced transparency in metamaterials," *Phys. Rev. Lett.* **101**(4), 047401 (2008).
29. A. A. Yanik, R. Adato, S. Erramilli, and H. Altug, "Hybridized nanocavities as single-polarized plasmonic antennas," *Opt. Express* **17**(23), 20900–20910 (2009).

1. Introduction

Metamaterials (MMs), as a new type of artificially structured materials, have been used to demonstrate exotic phenomena such as negative refraction [1, 2] and invisibility cloaking [3, 4]. Because metamaterials can provide extreme electromagnetic (EM) response to the incident light with the subwavelength resonating units, it becomes possible to achieve considerable electromagnetic response by just using a slab of metamaterial which is much thinner than a wavelength. For example, an ultra-thin metamaterial can be used to perfectly absorb light [5, 6] and to generate large optical chirality for polarization manipulation [7, 8]. Recently, such an approach has been extended to extreme phase control. By using an array of metamaterial units of structural parameters varying on a subwavelength scale, the light incident on an ultra-thin metamaterial can be bent by an angle using the phase discontinuity across the metamaterial, in a way that the Snell's law has been generalized on an inhomogeneous metamaterial surface [9–13]. In contrast to the ordinary spatial phase modulation devices employing liquid crystals [14, 15], the phase discontinuity is manipulated on a subwavelength scale (in the transverse direction) and is able to generate a larger bending angle through an array of metamaterial units of deep-subwavelength thickness. In the scheme, the wave front of the cross-polarized transmitted beam is greatly modified by a linear variation of the phase discontinuity which is provided by an array of plasmonic resonators. The large range of phase discontinuity (for the linear variation) is obtained by working at different regimes both near and far from the resonances through a series of plasmonic resonators. In fact, the phase variation across a resonance is always accompanied by the large variation of the amplitude. It is therefore challenging to obtain the desired phase variation with equal amplitude for the transmitted cross-polarized beam. In order to reconcile this dilemma between flexible phase control and equal amplitude, a double-resonance scheme for the plasmonic resonators was previously employed. While the resonances provide the flexible phase discontinuity, the two resonances work cooperatively to compensate each other so that the transmitted amplitude stays fairly constant for the whole series of plasmonic resonators. The scheme normally requires careful optimization of the structural parameters of the resonators [9, 10, 12, 13], and an accurate and efficient method has been developed in order to achieve the whole series of design [16]. Here, we investigate an alternative scheme in generating the phase discontinuity by an ultra-thin metamaterial constructed by an ensemble of the same type of anisotropic aperture antennas. In our design, all the anisotropic antennas have only one resonance at the same frequency in order to avoid the amplitude dispersion of the antennas working across resonance. We only need to engineer the orientation of the optical axes of the same type of

antennas at different positions on a subwavelength scale. By using a circularly polarized light (instead of linear polarization) impinging on the metamaterial, it can be completely converted to the cross-polarized light without the residual power in the original polarization, which can occupy larger than half of the transmitted power in the double-resonance scheme with linear polarization. Moreover, the phase control becomes intuitive that the spatial variation of the phase discontinuity has a simple linear relationship to the rotation angle of the optical-axis profile, as in one type of Q-plates [15]. Linear and parabolic phase variations for the optical-axis profile are investigated in order to bend or tightly focus the incident light near the diffraction limit.

2. Phase discontinuity through rotation of optical axes

In order to provide a full control of the wave front, it is essential to obtain the phase variation in the whole range from 0 to 2π , while sustaining the equal amplitude of the light from different positions. Here, we introduce an alternative framework (other than the double-resonance scheme) in modifying the wave front with the phase discontinuities through optical axis rotation. The approach is previously used for making a particular type of Q-plate (in generating an optical vortex and a topological charge) using a birefringent crystal plate with variable optical axis [14, 15]. Comparing to the Q-plate with birefringent crystals, metamaterial can generate a much larger difference of refractive indices between the two linear polarizations. It does not need a long interaction distance (e.g. in getting a half-wave plate) in the propagation direction and therefore the metamaterial can be much thinner than a conventional Q-plate. Another advantage is that by making metamaterial thinner than a wavelength, the interaction between neighboring pixels/cells arising from diffraction can be neglected, the original pixels of macroscopic size in a Q plate can thus be miniaturized down to the subwavelength scale. Therefore, subwavelength control of wave front now becomes possible (e.g. a larger bending angle or tighter focus shown in this work). For ease of discussion, we assume that the incident wave is a plane wave at normal incidence on the inhomogeneous metamaterial slab. The metamaterial has an array of aperture antennas, shown in Fig. 1(a), which are rotated at variable angles. The aperture antenna at zero rotation angle is shown in the upper panel of Fig. 1(a) with optical axis defined along the x -direction and y -direction, which are the two principal axes of the structure. Based on the similarity to the Q plate using a birefringent crystal plate, we therefore draw an analogy to the permittivity tensor in describing the different phase elapse for different linear polarizations. The thin aperture antenna unit can be described locally by using a homogeneous slab with deep

subwavelength thickness $h \ll \lambda$ and effective permittivity tensor $\hat{\epsilon} = \epsilon_0 \begin{pmatrix} \epsilon_1 & 0 \\ 0 & \epsilon_2 \end{pmatrix}$ using the

x - and y -polarization basis. Under normal incidence, as the x - and y -polarizations are decoupled, we use $t_1(t_2)$ to represent the complex transmission coefficient for the two linear polarizations respectively, i.e. the unit cell of the aperture antenna can be equivalently described by an effective medium with the same volume. For an aperture antenna with optical axis rotated by angle θ in the clockwise direction, the transmission coefficients can be represented using the Jones matrix in the basis of right-handed and left-handed circular polarization [7]:

$$\hat{t}(\theta)_{circular} = \begin{pmatrix} \frac{1}{2}(t_1 + t_2) & \frac{1}{2}(t_1 - t_2)e^{j2\theta} \\ \frac{1}{2}(t_1 - t_2)e^{-j2\theta} & \frac{1}{2}(t_1 + t_2) \end{pmatrix} \quad (1)$$

Now, suppose the incident plane wave is right-handed circularly polarized. The transmitted field \mathbf{E}_t is obtained by Eq. (1) as

$$\mathbf{E}_t = \frac{1}{2}(t_1 + t_2) \begin{pmatrix} 1 \\ 0 \end{pmatrix} + \frac{1}{2}(t_1 - t_2)e^{-j2\theta} \begin{pmatrix} 0 \\ 1 \end{pmatrix} \quad (2)$$

Therefore, if θ is spatially dependent, we can modulate the wave front for the cross-polarized light (left-handed polarized, the second term) by a spatially dependent phase discontinuity $e^{-j2\theta}$. The acquired phase discontinuity (phase gained by the incident light across the metamaterial) is twice that of the rotation angle of the antennas. This is a simple linear relationship between the phase discontinuity and the phase modulation (rotation angles) over the antennas array. We note that this phase discontinuity is not coming from the (frequency) dispersion by sweeping a series of resonating structure. The phase discontinuity here is geometric in nature and is related to the optical-axis rotation angle by a factor of two. Therefore, this scheme has an advantage that the phase discontinuity profile is broadband in nature and does not depend on the frequency at all. The polarization conversion efficiency can be defined in the form $\eta = |t_1 - t_2|^2 / (|t_1 - t_2|^2 + |t_1 + t_2|^2)$, and the transmission amplitude for the crossed polarized light is $|t_c| = 0.5|t_1 - t_2|$, furthermore, we can design metamaterial structures so that $t_1 + t_2 = 0$ is satisfied and the polarization conversion becomes 100%. In this case, there is no residual transmitted power in the original right-handed circular polarization. Only the cross-polarized light is transmitted with the designed phase discontinuity profile. The dispersion of the material will affect the transmission coefficients, so the polarization conversion efficiency η and transmission amplitude $|t_c| = 0.5|t_1 - t_2|$ for cross-polarized light are correspondingly influenced by the dispersion of the material.

Up to now, we could design and manipulate the output wave front though spatial rotation of the resonator arrays. As examples to demonstrate our proposal, we investigate two kinds of one dimensional phase profiles to demonstrate general manipulation of the wave front:

A: Linear phase discontinuity:

The generalized version of Snell's Law is in the form [9, 10, 12, 13]:

$$n_t \sin \alpha_t - n_i \sin \alpha_i = \frac{\lambda}{2\pi} \frac{d\Phi}{dx} \quad (3)$$

where α_i (α_t) corresponds to the incident (refraction) angle of the plane wave, n_i (n_t) is the refractive index in the incident (refracted) region. If we assume the plane wave is normally incident to the metamaterial surface, the refraction angle is governed by $\sin \alpha_t = (\lambda/2\pi)d\Phi/dx$, where the refractive index in the refracted region is assumed to be vacuum, i.e. $n_t = 1$. The linear phase variation, i.e. the gradient of the linear phase variation $d\Phi/dx$ being constant, can bend the incident wave at an angle. According to our scheme for the linear phase variation, the gradient of the phase variation is $k_G = d\Phi/dx = 2\pi/D$, where D is the total width of the antennas array and the rotation angle ranges from 0 to π .

B: Parabolic phase discontinuity:

In fact, the linear phase relationship is only one possibility to manipulate the wave front. As another representative example, as a one-dimensional variation, we can generate a phase discontinuity profile according to:

$$\Phi(x) = \frac{2\pi f}{\lambda} - \frac{2\pi\sqrt{f^2 + x^2}}{\lambda} \quad (4)$$

With such a parabolic profile, we can focus the incident light (wavelength λ) to a distance f beyond the metamaterial surface, where f is the focal length. Ordinary lens, e.g. a cylinder convex lens, accumulates the phase along the optical path with different thicknesses of

material. In contrary, we can generate such a phase discontinuity by an ultra-thin metamaterial surface in the subwavelength scale. Moreover, due to the abrupt phase control, we can focus the light to a tight focus near the diffraction limit as we will see later.

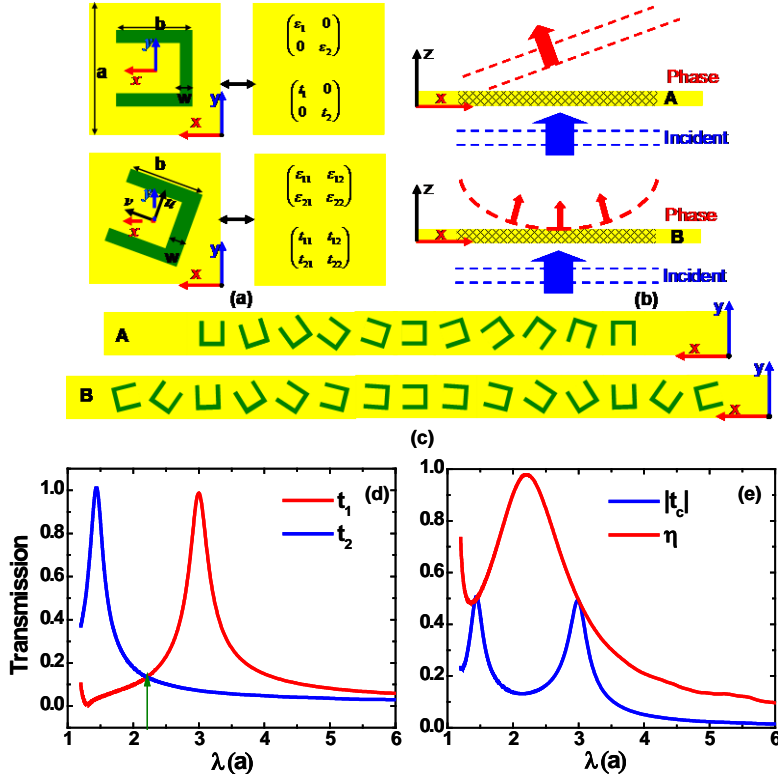


Fig. 1. Illustration of the phase transformation through structured metamaterial surface. (a) The unit cell geometric parameter for the metallic split ring aperture utilized here and its equivalent effective medium under rotation with their optical axis, the thickness of the metamaterial is $h = 0.2a$, the gap of the aperture $w = 0.1a$, and the side length of square aperture is $b = 0.6a$; (b) Light with well defined circular polarization (left-handed depicted here) gets scattered by the metamaterial surface, leading to the formation of the linear or parabolic phase variation at the output plane through rotating localized optical axes in a well designed manner, bending or focusing transmitted light according to the additional linear or parabolic phase discontinuity; (c) Schematic of the geometrical parameters of the structured surface investigated here. For structure A, the linear rotation is implemented, the position of each metallic aperture is at $x = na$, and the rotation angle is $\theta = 0.1n\pi$, where n is from -5 to 5 . For the structure B, the position of each metallic aperture is at $x = na$, and the rotation angle θ is related to the theoretical value according to Eq. (4) at that position, where n is from -7 to 7 . (d) The transmission amplitude of the effective medium with the unit of the metallic split ring aperture. (e) The polarization conversion efficiency and the transmission amplitude for the crossed-polarized light.

We have completed the schematic description, in the next step we need to design the subwavelength metallic antenna to realize the desired anisotropic EM response. Here, we adopt the split ring aperture antenna to realize the localized half-wave plate at a specific frequency, which is one of the most popular antennas investigated in the last decade [17–27]. With the geometric parameters defined in Fig. 1(a), the first resonance mode-mediated extraordinary optical transmission (EOT) effect occurs at the wavelength of $3.0a(5b)$ for the (linear) x -polarization, and the second resonance mode occurs at the wavelength of $1.4a(2.33b)$ for the y -polarization, shown in Fig. 1(d) with full-wave simulations. Between the two resonances, there exists a wavelength of $2.21a(3.68b)$, the transmission matrix element

fulfills the relation $|t_1| = |t_2|$, and $\arg t_1 = \arg t_2 + 1.09\pi \approx \arg t_2 + \pi$, the transmission of the antenna embodies the functionality of localized half wave plate in the sub wavelength region, where the transmitted field (nearly) does not contain the original polarized signal as discussed before. As depicted in Fig. 1 (e), the polarization conversion efficiency η and transmission amplitude $|t_c|$ for cross-polarized light are influenced by the dispersion of the metamaterial system. At the wavelength of $2.21a$ (equivalently $3.68b$), the polarization conversion efficiency η is about 98%, the transmission amplitude $|t_c|$ for cross-polarized light is about 13%. The low transmission amplitude for cross-polarized light results from the fact we obtain the nearly π phase shift for two orthogonal linear polarizations through resonance mechanism we adopt. We must point out that the full width of the half η is about $1.54a$, as shown in Fig. 1(e). Although the phase variation introduced by the antenna rotation is free of dispersion, i.e. broad bandwidth, the polarization conversion efficiency η and transmission amplitude $|t_c|$ are limited by the dispersion of the metamaterial system. At the first (second) resonance mode, due to the transmission coefficient $t_1(t_2)$ is nearly zero, while the transmission coefficient $t_2(t_1)$ is nearly one, the Jones matrix representing the transmission coefficients of the metamaterial is the same as the polarizer, each antenna could be viewed as a localized polarizer, the polarization efficiency at this wavelength is about 50%, as shown in Fig. 1 (e).

Taking into account of the linear and parabolic phase discontinuity along the metamaterial surface through an array of split ring aperture antenna with defined profiles of the rotation angles, as depicted in Fig. 1(c), one representative structure (A) is designed and is composed of 11 rotating antennas to realize the linear phase variation from 0 to 2π . Considering the finite size of the unit cell, the phase variation is not continuous but is discrete. For structure A, each unit cell only needs a discrete rotation with step size of 0.1π to realize the linear phase variation from 0 to 2π . The case of structure B contains 15 rotating resonators with defined rotation angle to realize the parabolic phase variation in Eq. (4). Here, we emphasize that phase variation acquired by rotating optical axis is free of dispersion of the resonator, as we could keep the desired anisotropic behavior.

To verify our proposed scheme, we have performed full-wave simulations using CST Microwave Studio, based on the finite difference time domain (FDTD) algorithm [28]. We utilize the perfect conductor approximation (PCA) for simplicity. The results presented here can be extended to other frequency regimes, when the dispersion of metal is taken into consideration. We focus on the wavelength $\lambda = 2.21a(3.68b)$, where the element of transmission matrix fulfills $t_1 = -t_2$. In the y direction, we adopt periodic condition, while in the x direction, perfectly matched layer absorbing boundary condition is adopted. We set the mesh size to be $0.01a$ - $0.02a$ in the transverse direction and $0.02a$ - $0.05a$ in the longitudinal z direction. The mesh size with high precision enables us to model the array of the metallic apertures exhibiting inhomogeneous and anisotropic EM responses with high accuracy.

3. Light bending through phase discontinuities across an ultra-thin metamaterial surface

As depicted in Fig. 1, a representative structure (A) with 11 rotating resonators in order to realize the linear phase variation from 0 to 2π . Under the normal incidence, we investigate the bending phenomenon for both left and right-handed circular polarizations. As depicted in Fig. 2(a), under left handed circular polarization incidence, the transmitted field acquires an additional wave vector along the interface induced by the artificial patterned surface, and the bending angle could be deduced from the phase matching at the interface by $\sin \alpha_r = -(\lambda/2\pi)d\Phi/dx = -\lambda/(11-1)a = -0.22(\alpha_r = -12.71^\circ)$, where the plane wave is assumed in the form $e^{i(\omega t - \mathbf{k} \cdot \mathbf{r})}$. The angle of the refracted light in the far field is -13° , as shown in Fig. 2(c), agreeing well with the theoretical description. As we discussed before, the

transmitted light only contains the bent cross-polarized light (right-handed circular polarization), the original polarized light (left handed circular polarization) vanishes. For right handed circular polarization incidence, shown in Fig. 2(b) and 2(d), the bending angle of the cross-polarized light (left-handed circular polarization) is $12.71^\circ(13^\circ)$, while the direction is opposite to the case of the left-handed circular polarization incidence. The bending phenomenon is related to the incident circular polarization. Especially, for left-handed circular polarization incidence in the range of $\alpha_i = 0$ to $12.71^\circ(13^\circ)$, the metamaterial interface exhibits negative refraction, while for right-handed circular polarization incidence in the range of $\alpha_i = -12.71^\circ(-13^\circ)$ to 0 , the metamaterial interface exhibits negative refraction as well.

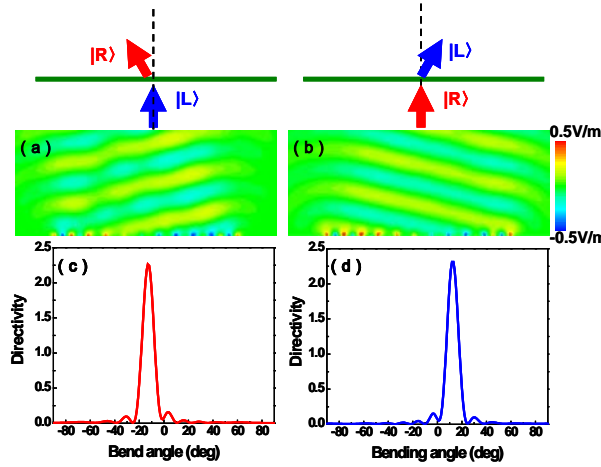


Fig. 2. Illustration of the additional linear phase discontinuity through structured metamaterial surface. One of the electric field component(x) distributions for the left-handed circular polarization incidence (a) and right-handed circular polarization normal incidence (b) indicate the wave front across the resonator interface induced by the additional wave vector contribution. The far field directivity illuminates the bending phenomenon due to the induced linear phase discontinuity through rotating optical axis for left-handed circular polarization incidence(c) and right-handed circular polarization incidence (d).

4. Tight Light Focusing through phase discontinuities across an ultra-thin metamaterial surface

To further demonstrate the feasibility of the additional phase discontinuities in our scheme, we modulate the metamaterial surface to focus the incident plane wave through additional convex phase discontinuity. According to Eq. (4), the interface is created by arranging 15 antennas at various angles, as shown in Fig. 1. As viewed in the Fig. 3(a) and 3(e), for left-handed circular polarization incidence, we can create a converging wave front; while for right-handed circular polarization incidence, we can create a diverging wave front. The focusing (defocusing) behavior of the metamaterial surface can also be viewed in the electric field energy density distribution, see Fig. 3(c) and 3(g), the focus length (f) is $f = 10a$, which is slightly different from the targeted focus length $f = 11a$ in Eq. (4). The full width of the half maximum energy density is $w = 0.77\lambda$ for left-handed circular incidence, which is in the region of tight focus in the far field focusing. In contrary, the transverse energy density distribution does not concentrate energy for the incident light of right-handed circular polarization, the transverse energy density becomes broad in the entire transverse region, shown in Fig. 3(g), due to the introduced diverging wave front through the metamaterial. Visual understanding of the EM evolution through the metallic resonator arrays can be obtained by formulating the \mathbf{E} field after the metallic surface. When the left-handed circular

polarization is normally incident, the transverse \mathbf{E} field at the observation plane can be approximately described by

$$\mathbf{E} = A \sum_i^n r_i^{-1} e^{-jk_0 r_i} e^{j2\theta_i} (1, -i)^T \quad (5)$$

where r_i is the distance between the i th aperture element to the observation point, A is the scale factor to reveal the transmission behavior of each unit, and the field at the observation point is the summation of the contribution from each aperture element. The phase associated with the incident polarization state leads to the optical spin dependent phenomenon in our proposed metamaterial structures [14]. The analytical prediction could map the main feature of the numerical results, as shown in Fig. 3(b), 3(d), 3(f), 3(h), where the displayed region in analytical description is from $2a$ to $20a$ along the z direction. By far, we can model the most representative parabolic phase to realize the convex or concave wave front through rotating the optic axes of the antennas investigated, which is different from conventional optical components, where the spatial phase profile relies on light propagation over different optical lengths.

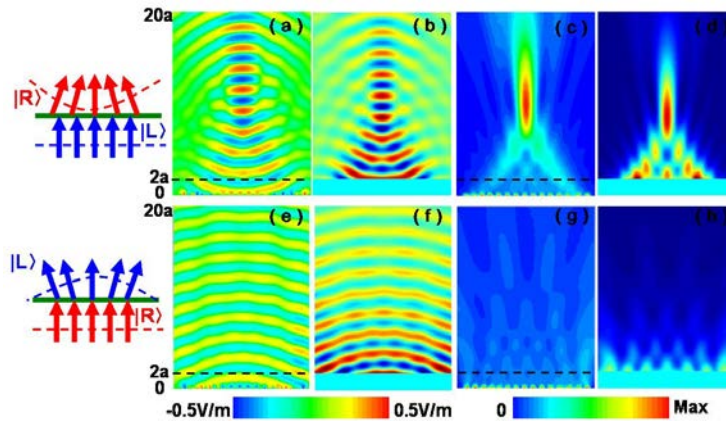


Fig. 3. Numerical and theoretical illustration of the additional parabolic phase discontinuity through structured metamaterial surface. The region exhibiting the numerical results is from 0 to $20a$ along the z direction, and the region of the theoretical results is from $2a$ to $20a$ along the z direction, where the transverse direction is from $-8a$ to $8a$. One of the electric field component(x) numerical and theoretical distributions for the left-handed circular polarization incidence (a), (b) and right-handed circular polarization normal incidence (e), (f) indicates the convex and concave wave front across the resonator interface. The corresponding theoretical results are The numerical and theoretical electric field energy density illuminates the focusing (defocusing) phenomenon due to the induced convex phase discontinuity through rotating optical axis for left-handed circular polarization incidence(c), (d)and right-handed circular polarization incidence (g),(h).

5. Conclusion

We have proposed an ultra-thin metamaterial constructed by an ensemble of the same type of anisotropic aperture antennas with phase discontinuity for wave front manipulation across the metamaterial. The phase discontinuity only depends on a precise control of the optical-axis rotation profile of the antennas on a subwavelength scale, in which the rotation angle of the optical axis has a simple linear relationship to the phase discontinuity. By simply manipulating the rotation of the optical axes, an abrupt beam bending (linear phase variation case) and tight focusing (parabolic phase variation case) across the ultra thin metamaterial are numerically demonstrated. Such a simple approach enables effective wave front engineering within a subwavelength scale. Our proposal would enrich the functionality of the state-of-art metamaterial design, illuminates new ways in designing metmaterials, and the exotic EM

response generated would encourage the precise manipulation of the light in the subwavelength region [29].

Acknowledgment

This work was supported by Hong Kong Research Grants Council (GRF grant CityU 102211 and Project No. HKUST2/CRF/11G). This work is also supported by the 973 Program of China under Grant No. 2012CB921900 and the National Natural Science Foundation of China under Grants 10934003.